Influence of oxygen ions irradiation on the optical properties of photoanodes for dye sensitized solar cell

Amrik Singh[1*], Devendra Mohan[2], Dharmavir S. Ahlawat[1], Sandeep Chopra[3]

[1]Material Science Lab., Department of Physics, Chaudhary Devi Lal University, Sirsa, Haryana 125055, India
[2]Laser Laboratory, Department of Applied Physics, Guru Jambheshwar University of Science &Technology, Hisar 125001, Haryana, India
[3]Inter-University Accelerator Centre, New Delhi 110067 (India)

[*]Corresponding author, E-mail: amrik23kuk@gmail.com

Received: 09 March 2016, Revised: 26 September 2016 and Accepted: 03 November 2016

DOI: 10.5185/amlett.2017.6518
www.vbripress.com/aml

Abstract

Indium Tin Oxide (ITO) coated glass acts as a substrate for photoanode of Dye Sensitized Solar Cells (DSSCs). The ITO substrate was irradiated by oxygen ion with different fluence ($1x10^{11}$ and $1x10^{12}$ ions/cm^2) at 100 MeV energy. The TiO_2 films were also subjected with same ion irradiation at 100 MeV of energy with fluence of $1x10^{11}$ ions/cm^2 and $5x10^{12}$ ions/cm^2. At 100 MeV energy of O^{7+} ion the electronic and nuclear energy loss for TiO_2 film have been measured $7.38x10^{-1}$ KeV/nm and $3.8x10^{-4}$ KeV/nm respectively. However, the electronic and nuclear energy loss of ion irradiation for ITO substrate were $7.4x10^{-1}$ KeV/nm and $4.06x10^{-4}$ KeV/nm respectively. Similarly longitudinal/ lateral straggling of ITO and TiO_2 have been found 3.87 μm/2.50 μm and 3.62 μm/1.14 μm respectively. Further, the structural and optical properties of these samples were monitored by X-ray diffraction (XRD), scanning electron microscopy (SEM) and UV-visible spectroscopy. It was found that oxygen ion (O^{7+}) irradiation of ITO film has slightly changed the crystallinity and transmission decreases. Furthermore, the particle size of TiO_2 thin film has been obtained 80 nm corresponding to (101) plane of XRD pattern. In the case of ITO thin film the crystallite size and band gap changes from 62.35 nm to 53.89 nm and 3.993 eV to 3.971 eV at $1x10^{12}$ ions/cm^2 respectively. Moreover this paper is also reporting that irradiation by swift heavy ion has changed the transmission of the ITO films, and its values decreases as compared to pristine (ITO) which degraded the performance of DSSC. Consequently, a very small value of absorbance is reported for ITO film. However, the absorbance of TiO_2 film has found to increase with irradiation of oxygen ion at fluence of $1x10^{12}$ ions/cm^2 and decreased at $5x10^{12}$ ions/cm^2. It is also confirmed that the absorbance of TiO_2 film and TiO_2/ITO photoanode increases with irradiation of oxygen ion at fluence of $1x10^{12}$ ions/cm^2 and decreased at $5x10^{12}$ ions/cm^2. The band gap values of TiO_2 thin film were obtained to have a change from 3.37 eV (for pristine) to 3.44 eV at $5x10^{12}$ ions/cm^2. But the decrease in band gap is also found 3.17 eV at fluence of $1x10^{12}$ ions/cm^2. However, N719 dye loaded O^{7+} ($1x10^{12}$ ions/cm^2) irradiated TiO_2 film show high absorption as compared to other samples. Thus the dose of O^{7+} irradiation at fluence $1x10^{12}$ ions/cm^2 may fabricate more efficient DSSC and consequently future prospective of such type of photoanode materials for dye sensitized solar cells seems to be bright.

Keywords: Swift heavy ion irradiation, energy losses, dye sensitized solar cells, optical properties of TiO_2 /and ITO thin films, TiO_2 / ITO photoanode.

Introduction

Dye sensitized solar cells (DSSCs) have attracted the researchers due to their low cost, easy fabrication, eco-friendly and high performance **[1-2]**. The DSSCs consist of a photoelectrode, counter electrode, electrolytes and transparent conducting oxide (TCO) substrate on which dye adsorbed semiconductor oxide layer is coated. The highly transparent ITO (indium doped tin oxide) thin films are having their use in many optoelectronics devices including DSSC. The ITO is a transparent conducting oxide material act as a substrate for the coating of the TiO_2 thin films in DSSC which act as photoanode for DSSC **[3-5]**. However, the TiO_2 material has been used in various applications like sensors, antireflection coating, and thin film devices and solar cells **[6-11]**. The properties of TiO_2 has been investigated by many researchers **[12]** due to its high refractive index, low cost, non-toxicity, good radiation resistance, conversion of light energy into electrical energy and large number of other technological applications. Promising materials have been developed by modification in the structural and

optical properties using advance techniques **[13**, **14]**. Swift heavy ions (SHI) is an advance technique can be used to modify properties of materials for development of technologically suitable new type of materials after preparation of thin film, powder material and bulk form materials. The SHI irradiations is an effective technique for desired modification in the material properties by controlling various parameters of ion beam as like energy, mass of the ion, oxidation state of the ion, atmospheric or other pressure, temperature during irradiation and dose of ions. The change in structural, electrical, magnetic and optical properties of the materials has been investigated by the interaction of high energy ion with atoms of the target material and thus produce a unique material with novel properties which cannot be generated by other methods **[15]**. The transmittance of ITO sample irradiated by Ni^{8+} ion was reported to be increased by 13% as compared to pristine sample which is a very favorable result for applications in DSSC. However, the electrical resistivity of the sample was found to be decreased with SHI irradiation [**16**]. The modification in electrical and optical properties have been confirmed in molybdenum doped indium oxide thin films irradiated by O^{7+} swift heavy ion [**17**]. At high energy of the ion beam electronic energy loss is found dominant over nuclear energy loss. The nature of target material also alters the loss of energy inside the material, creation of disorderness, amorphization, recrystallization inside the target material and positively charged ions creates along the ion path to produce a cylinder of ions [**18-22**]. Thus the effect of SHI has been observed different in the case of different target materials; it means that the same ion at a constant energy penetrates into two different materials with the different energy losses and depth range. Moreover, novelty of this technique is for modification in material properties that energetic ion beam offers much broader range of possibilities as compared to the ion implantation **[23-29]**. For a case, SHI irradiation of ITO and TiO_2 photoanode may have possibility to open new avenues for unique optical, structural and electrical properties that could be helpful in research and industry related to renewable energy sources with broad application perspectives. Our main objective is to investigate the effect of SHI irradiation on the properties of synthesized desirable photoanode material for DSSCs. Hence, in the present course of work a sol-gel dip coating technique has been used to produce homogenous thin films of TiO_2 on ITO substrate at low cost. Moreover, optical and structural properties have also been investigated for pristine as well as O^{7+} ion irradiated ITO and TiO_2 thin film samples.

Experimental

Materials used

Titanium isopropoxide (TTIP, Sigma Aldrich > 97%) and glacial acetic acid (Acetic acid glacial, ≥99.85%), 3050 Spruce Street, Saint Louis, MO 63103, USA, ethanol (Merck Absolute, USA).

Method of samples preparation

The TiO_2 thin films of desirable quality were synthesized successfully by sol-gel dip coating technique. Now a 4 mL glacial acetic acid, 60 ml ethanol as solvent and 2 mL deionized water were mixed together to form a solution A. Then 10 mL TTIP in ethanol conical flask was taken and solution A was poured into the stirred TTIP drop wise. After 8 hours continuous stirring at room temperature (30 ^oC) we obtain a clear and transparent sol. The reaction between Titanium alkoxide and water proceeds according to following reactions **[30]**:

$$Ti\,(OR)_4 \;+\; 2H_2O \;=\; TiO_2 + 4ROH \qquad (1)$$

The thickness of thin film was obtained as 190 nm. The solution was putted at room temperature before coating. Indium tin oxide thin film coated glasses were used as transparent conducting substrate. The TiO_2 sol was coated onto ITO glass by a dip coater (MTI Corporation). The dipping speed has been adjusted at 10 inch/min. There after each sample was heated at 100 ^oC upto 10 minutes for removal of extra solvents. This process was repeated carefully four times for obtaining desired thickness of TiO_2 films. Finally all the films coated substrate were annealed at 450 ^oC upto one hour.

SHI irradiation of samples

The TiO_2 films were irradiated with different fluence of $1x10^{12}$ ions/cm^2 and $5x10^{12}$ ions/cm^2 of O^{7+} ion having an energy 100 MeV using 15 UD Pelletron Tandem Accelerator at Inter-University Accelerator Centre (IUAC) New Delhi, India. For track formation the threshold energy values of O^{7}+ beam irradiation energy for ITO and TiO_2 were found 2.2 MeV and 2.45 MeV respectively **[30]**. The ITO as substrates was irradiated with oxygen ion at 100 MeV energy to have fluence $1x10^{11}$ ions/cm^2 and $1x10^{12}$ ions/cm^2. Further the TiO_2 films were irradiated by the same ion with 100 MeV energy at fluences of $1x10^{12}$ ions/cm^2 and $5x10^{12}$ ions/cm^2. The vacuum in the irradiation chamber was fixed at ~10^{-6} Torr and ion beam current was kept constant at 1 pnA (particles nano ampere). The focused oxygen ion beam was scanned over the sample area 1x1 cm^2 of ITO / TiO_2, at this high energy the ion suffers electronic (inelastic) collisions inside the target material. The electronic and nuclear energy losses at 100 MeV oxygen ion were calculated by using SRIM 2013 Software **[31]**.

$$T = \frac{\mathrm{fxA}}{\mathrm{Ix6.25x10^9}} \qquad (2)$$

where, f is fluence (ions/cm^2), T is time for irradiation of target material, A is scan area of sample (cm^2) and I is the beam current in pnA, where pnA is paticle nano ampere.

In our experiment the beam current was taken as one pnA. It may be also explained that current is divided by charge state which means each particle/ ions carry electronic charge equivalent to its charge state. The time

required in both the samples for dose $1x10^{11}$ ions/cm^2, $1x10^{12}$ ions/cm^2 and $5x10^{12}$ ions/cm^2 was 16 sec, 160 sec. and 760 sec respectively.

Characterization techniques

The irradiated and pristine samples were characterized by using various experimental techniques.

X-ray diffraction

The structural analysis of prepared thin films was performed by using XRD set up (Panalytical's X'Pert Pro, 0º-160º). The radiation used is CuKα whereas nickel metal is used as beta filter) at a wavelength of 1.541Å. The angle of incidence for x-ray beam was taken 2º/min., SAIF, PU, Chandigarh.

UV-Visible Spectroscopy

The UV-Vis spectra was also carried out by using a UV-Visible spectrophotometer, model no. Varian Cary-5000. Wavelength range 300 to 80 nm.

Results and discussion

Energy losses of oxygen ion irradiated ITO and TiO_2 thin films

Interaction of O^{7+} with ITO can be categorized as a low ion and high ion beam velocity. At low energy (velocity) of ion beam its equilibrium ionic charge decreases as it starts to capture an appreciable number of electrons and charge neutralization process of the ion is nearly completed then the collision between ion and target material is an elastic type. The elastic type collision (S_n) become dominant over the inelastic collisions (S_e). However with the increase in energy of oxygen ion (100 MeV) the electronic energy losses (dE/dX_e) increases and nuclear energy loss decreases (dE/dX_n) **[31-33]**.

The electronic and nuclear energy loss (keV/nm) for oxygen ion irradiation on ITO film are obtained $7.14x10^{-1}$ and $4.06x10^{-4}$ keV/nm respectively at 100 MeV of beam energy as shown in **Fig. 1a**. The longitudinal and lateral range straggling values were obtained 3.87 μm and 2.50 μm at 100 MeV of energy respectively. However longitudinal range straggling was calculated low as compared to lateral straggling in the case of below 45 MeV of the ion energy and after this its values increases sharply as compared to lateral straggling **[30]**. SHI transfer energy to the lattice is a two-step thermodynamic process (i) evolution of energy within the target electron via electron - electron interaction and (ii) energy transfer between electron and lattice atom via electron - phonon coupling. This energy transfer leads to increase in local temperature that can reach the melting temperature of semiconductor oxide resulting in formation of highly disordered or amorphized latent tracks after ultrafast quenching of the molten matter The incoming ions deposit their energy onto the target electrons in atoms. The electrons are then ionized, leaving behind a zone of ionized cores which creates coulomb repulsion, leading to the explosion of the ions and form cylindrical zone in the material **[34]**.

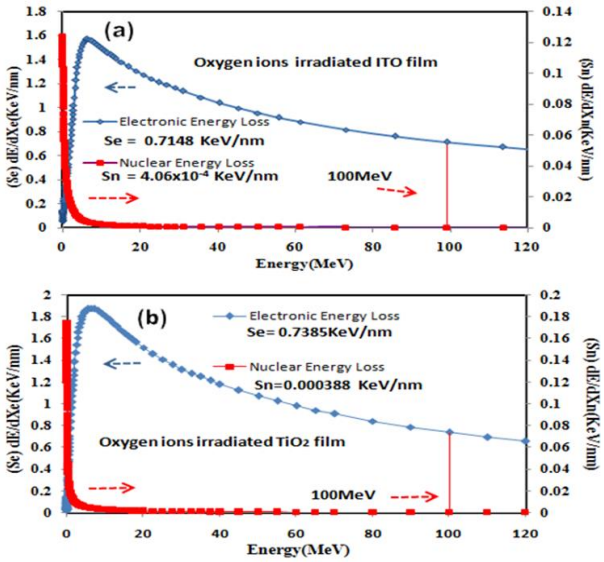

Fig. 1. (a) Electronic and nuclear energy losses of oxygen ion in ITO film, (b) Electronic and Nuclear energy losses of oxygen ion in TiO_2 film.

Fig. 1b demonstrates that in the case of TiO_2 film on passage of O^{7+} the S_e and S_n values were found $7.385x10^{-1}$ keV/nm and $3.88x10^{-4}$ keV/nm respectively. The longitudinal and lateral straggling for O^{7+} irradiated TiO_2 thin film are obtained 3.62 μm and 1.41 μm respectively. If more is the ion spread in a rambling way then higher energy will be deposited by the ion into the target material. Thus width of ion distribution and projected range depend on the lateral and longitudinal range straggling of the ion. Moreover, there is a difference in the scattering of heavy and light ions and hence range straggling will be different for both types of ions.

XRD analysis of ITO thin films

Fig. 2 shows the XRD pattern of ITO (indium tin oxide) thin films substrate in pristine form along with other two samples irradiated with oxygen ion fluence $1x10^{11}$ ions/cm^2 and $1x10^{12}$ ions/cm^2 at energy 100 MeV. The pristine peaks are found corresponding to planes (211), (222), (400) (440) and (622) at 2θ values 21.358º, 30.194º, 35.254º, 50.612º and 60.134º respectively. The 2θ value for highest peak of pristine was observed at 30.194º while for other two samples irradiated with O^{7+} ion the peaks were found at slight different positions with 30.283º and 30.357º corresponding to the highest intensity which are also given in the **Table 1**. The highest intensity peak corresponds to (222) plane for all the three samples. With the increase in fluence by $1x10^{12}$ ions/cm^2 the peak (222) of pristine shifted from 30.194º to 30.357º. Similarly a slight difference of respective peak's intensity was also observed. The crystallinity of the film degraded with ions irradiation which can be seen more clearly for smaller peaks corresponding to plane (622) for the ITO sample irradiated at $1x10^{12}$ ions/cm^2. A similar behavior

was also reported by other researchers **[16**, **35-38]**. Moreover a close comparison of all the peak's intensity was found in decreasing order as we move from pristine to the sample at $1x10^{11}$ ions/cm^2 and then sequentially for the sample at $1x10^{12}$ ions/cm^2. A careful examination of the XRD patterns of ITO further reveals that the there is a further decrease in intensity of (222) peak at dose $1x10^{12}$ ions/cm^2 more as compared to the sample irradiated with fluence of $1x10^{11}$ ions/cm^2.

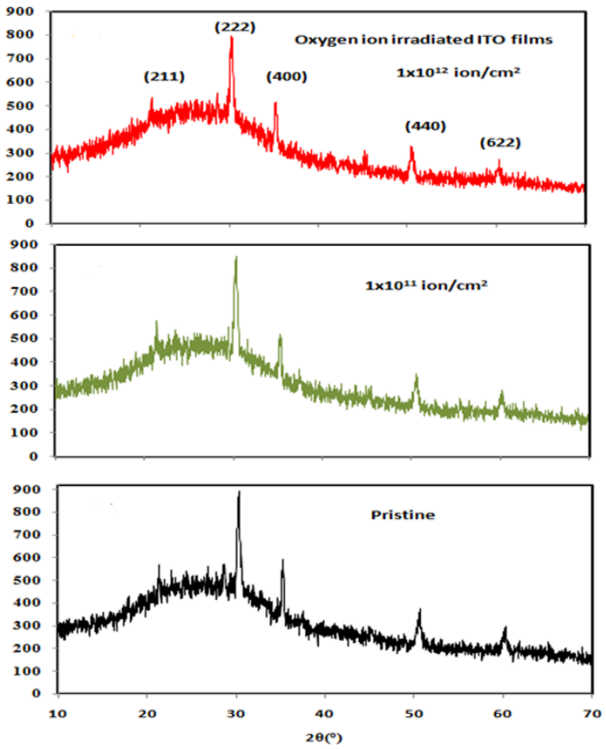

Fig. 2. XRD pattern of the oxygen ion irradiated ITO film.

The lattice constant (222) decrease with increase in fluence of oxygen upto $1x10^{12}$ ions/cm^2 and calculated by relation (3)

$$d = \frac{a}{\sqrt{h^2+k^2+l^2}} \quad (3)$$

where, d is inter planar spacing, a is lattice constant and hkl is Miller indices.

The different crystallite size (D) of the ITO thin films are given in the **Table 2** corresponding to highest intensity peaks for the XRD pattern of ITO. The crystallite size was calculated by using Debye Scherer formula [**25**]

$$D = \frac{k\lambda}{\beta Cos\theta} \quad (4)$$

where, k is the structure factor, λ is the X-Ray wavelength, β is the full width at half maxima, θ is the Brag Diffraction angle. From the **Table 2** reduction of particle size confirm XRD peak broadening shown in **Fig. 2**. The peaks broadening seem to be maximum at a dose of $1x10^{12}$ ions/cm^2 for the smallest particle size 53.89 nm as compared to their respective values for pristine.

Optical properties of ITO thin films

The transmission of ITO film was found at approximately 90-95% in the wavelength range of 300-800 nm shown in **Fig. 3a**. The transmission of the thin film decreases with increase in fluence of oxygen ion at 100 MeV. The reduction in transmittance of the film is due to incorporation of defects **[33**, **34]**. The transmittance of the ITO film depends on the oxygen concentration, at $1x10^{11}$ ions/cm^2 and $1x10^{12}$ ions/cm^2 dose of oxygen ion **[39]**. On the basis of results the decrease in the transmission of ITO film was found 85-90% for $1x10^{12}$ ions/cm^2

Table 1. Various parameters of Oxygen ion irradiated ITO film.

Samples	ITO	ITO	ITO
Dose (ions/cm^2)	Pristine	$1x10^{11}$	$1x10^{12}$
2θ(°) (211)	21.358	21.329	21.230
d spacing (Å) (211)	4.1552	4.1611	4.1814
2θ (°) (222)	30.194	30.283	30.357
d spacing (Å) (222)	2.9582	2.9498	2.9428
2θ(°) (400)	35.254	35.295	35.190
d spacing (Å) (400)	2.5444	2.5437	2.5489
2θ (°) (440)	50.612	50.575	50.488
d spacing (Å) (440)	1.8025	1.8038	1.8071

Table 2. Various parameters of oxygen ion irradiated ITO film.

Sample	Dose (ions/cm^2)	FWHM (radian)	Crystallite Size D (nm)	Direct band Gap (eV)	Interplanar Spacing d(Å) (222)	Lattice constant(Å)
ITO	Pristine	0.138	62.35	3.993	2.9582	10.2472
ITO	$1x10^{11}$	0.152	56.76	3.981	2.9498	10.2181
ITO	$1x10^{12}$	0.159	53.89	3.971	2.9428	10.1938

irradiated samples as compared to pristine and $1x10^{11}$ ions/cm^2 irradiated sample. V. Kumar *et al.* **[39]** and Gokulkrishanan *et al.* **[17]** have reported a similar variation in transmittance of semiconductor oxide film with oxygen ion irradiation. The absorbance of the ITO film was obtained very low which desirable as a substrate for a solar cell in the optical region.

$$\alpha h\nu = A(h\nu - Eg)^m \quad (5)$$

where, A is a constant depends on transition probability. The band gap was calculated from the plot between $(\alpha h\nu)^{1/m}$ and photon energy($h\nu$) **[38]**, m=1/2 for direct band and m=2 for indirect band gap. However in our case the direct band gap is observed. The absorption coefficient α was calculated from equation (6)

$$\alpha = \frac{1}{t}\ln\left(\frac{1}{T}\right) \quad (6)$$

where, t is thickness and T is the transmission of the thin film and **Fig. 3b** has been plotted by use of data values of transmission given in **Fig. 3a**. Thickness of thin films was measured 1000 Å.

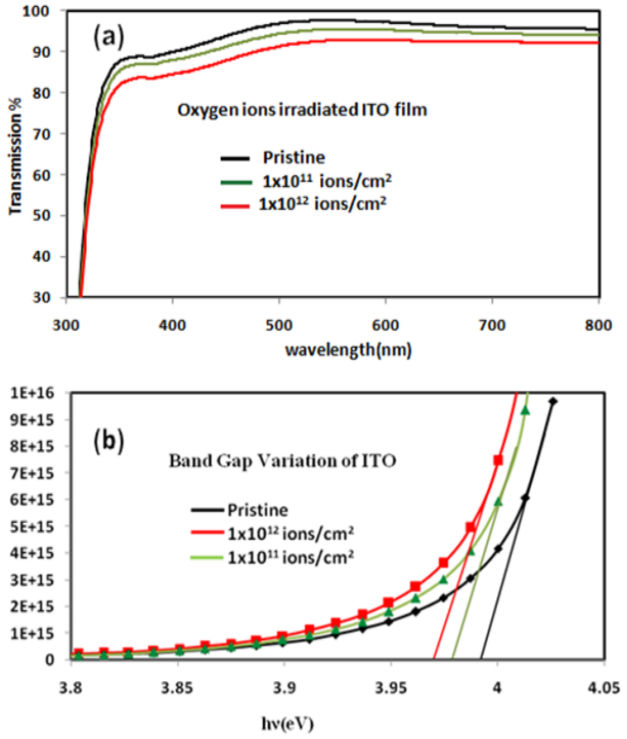

Fig. 3(a) Transmission of oxygen ion irradiated ITO thin films and **3(b)** band gap variation of oxygen ion irradiated ITO thin films.

The band gap of thin film samples were obtained 3.993 eV, 3.981 eV and 3.971 eV corresponding to pristine, $1x10^{11}$ and $1x10^{12}$ ions/cm^2 fluences of samples respectively as shown in **Fig. 3b**. The 100 MeV oxygen ions has changed the band gap of indium tin oxide (ITO) film. The structural and optical parameters of the pristine and ion irradiated ITO films have been given in the **Table 2**. The slight decrease in band gap energy with increase in ions irradiation was found and similar results are also reported by earlier investigators **[37, 38]**. However there is a small band gap change which is found at the second and third decimal place after irradiation of the ITO thin film at different fluences. The decrease in band gaps may be due to creations of energy levels close to the conduction band **[39]**.

The band gap values of oxygen io

XRD Analysis of TiO_2 thin film

Fig. 4 demonstrates the XRD pattern of pristine TiO_2 thin film in anatase and rutile phases coexist in a sample which shows high intense peak corresponding to plane (101) for anatase phase. But the XRD peaks are found small for rutile phase as compared to anatase phase. The XRD pattern confirm high crystalline nature of the anatase phase prepared sample of TiO_2. As the rutile and anatase phases co-exist in the same TiO_2 pristine sample. The particle size was found 80 nm corresponding to (101) plane of anatase phase structure. The XRD planes (101), (103, (004), (112), (200), (105), (211) and (110), (101) are obtained corresponding to anatase and rutile phase respectively.

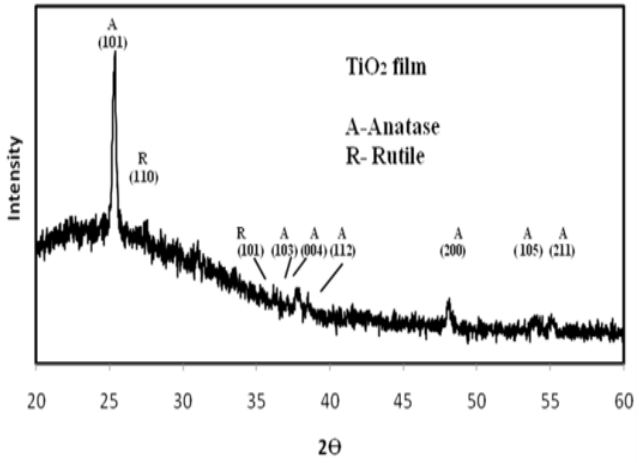

Fig. 4. XRD pattern of pristine TiO_2 film.

Optical properties of TiO_2 thin films

The absorbance of TiO_2 and TiO_2/ITO glass in the wavelength range of 300-800 nm has been shown in the **Fig. 5a** and **Fig. 5b** respectively. The pristine TiO_2 film has 3-25% absorbance in the wavelength range from 375-800 nm. The O^{7+} ion irradiation has modified absorbance of the films. Furthermore at $1x10^{12}$ ions/cm^2 the absorbance of the TiO_2 thin films is found to be increased and at high fluence of $5x10^{12}$ ions/cm^2, it has decreased.

The decrease in absorption may be because of increase in oxygen contents of the films. The concentration of oxygen altered the absorbance of thin films **[18]**. However many researchers have also reported the depletion of oxygen with ion irradiation **[38-41]**.

The plot of Fig**. 5c** is showing the band gap variation of TiO_2 thin film samples. Band gap of the irradiated films of thickness 190 nm has decreased from 3.37 eV (pristine) to 3.17 eV at $1x10^{12}$ ions/cm^2 fluence and again increased

to 3.44 eV at a dose of $5x10^{12}$ ions/cm^2. Our results are found well matched as reported by other workers **[29**, **32]**. This decrease in the band gap may be believed due to many body defects. The increase in band gap of the material at high fluence of $5x10^{12}$ ion/cm^2 is also reported earlier due to MB shift **[37]**.

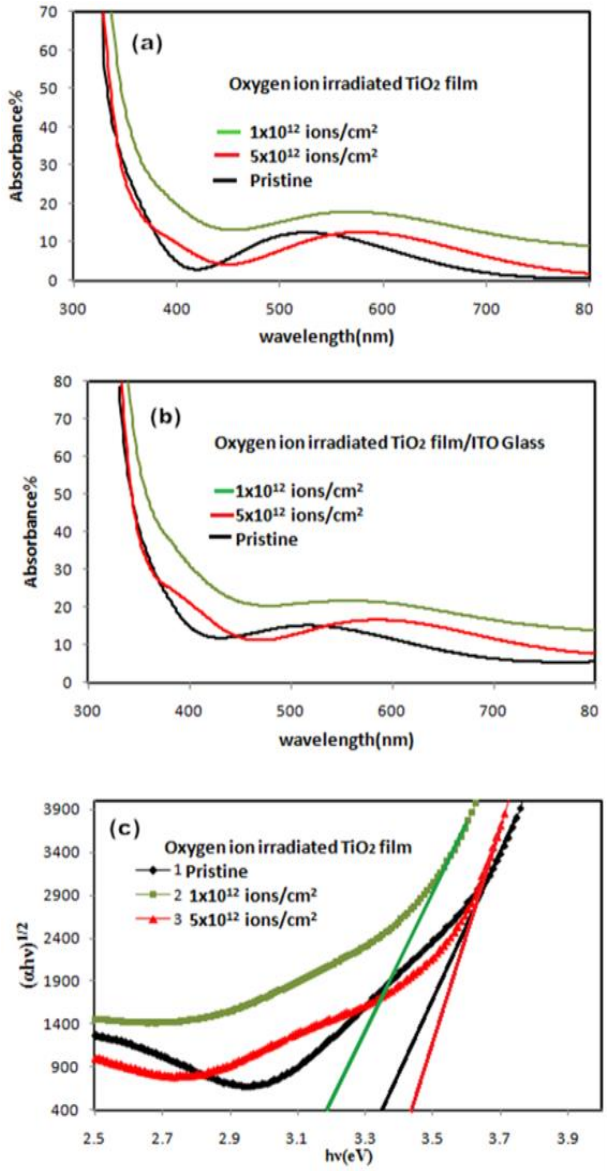

Fig. 5. (a) Absorbance of O^{7+} ion irradiated TiO_2 thin films, **(b)** Absorbance of oxygen ion irradiated TiO_2 film/ITO glass and **(c)** Band gap variation of TiO_2 thin films.

Dye adsorbed ion irradiated samples of TiO_2

The absorbance of N719 dye loaded ion irradiated samples of TiO_2 is also showing in **Fig. 6**. The absorption of dye desorbed ion irradiated samples was found to increase as compared to pristine TiO_2 samples.

The $1x10^{12}$ ions/cm^2 ion irradiated sample show high absorbance value as compared to other dye loaded samples. The highest value of absorption for $1x10^{11}$ ions/cm^2 dose irradiated sample was due to more adsorption of dye as compared to other samples. Furthermore the absorbance of dye loaded thin film of TiO_2 was found to increase for $1x10^{12}$ ions/cm^2 ion irradiated sample and again has decreased in a sample for a dose of $5x10^{12}$ ions/cm^2.

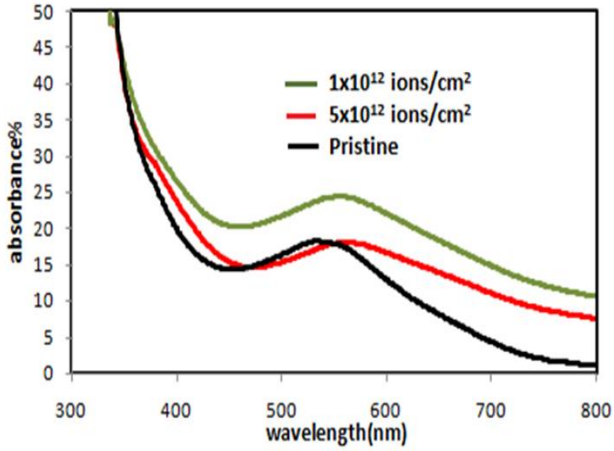

Fig. 6. Absorbance of N719 dye loaded ion irradiated TiO_2 thin films.

Conclusion

The XRD patterns of ITO and TiO_2 thin films confirmed crystalline semiconductor nature of the synthesized samples. The process of electronic energy loss (S_e) was found dominant over nuclear energy loss (S_n) at high energy 100 MeV of oxygen ions O^{7+} irradiation for both type of samples under study. The S_e and S_n corresponding to TiO_2 thin film substrate are found $7.38x10^{-1}$ kev/nm and $3.8x10^{-4}$ keV/nm respectively. But the values of S_e and S_n for ITO have been obtained $7.14x10^{-1}$ keV/nm and $4.06x10^{-4}$ keV/nm respectively. In the optical properties, the band gap for oxygen ion irradiated ITO thin films have been obtained to decrease from 3.993 eV to 3.981 eV at $1x10^{11}$ ions/cm^2 and further decreases to 3.971 eV for a sample at $1x10^{12}$ ions/cm^2. For the structural characterization the crystallite size of ITO was found to decrease from 62.35 nm (pristine) to 53.89 nm of a sample with the oxygen ion fluence at $1x10^{12}$ ions/cm^2 for energy 100 MeV. In the case of TiO_2 thin film, the XRD analysis confirmed crystalline nature of the material and its particle size is reported 80 nm. It has also been observed that the absorbance of TiO_2 film increases with irradiation of oxygen ion at fluence of $1x10^{12}$ ions/cm^2 and decreases at $5x10^{12}$ ions/cm^2. Moreover, the band gap values of TiO_2 thin films corresponding to one pristine sample and two samples at irradiation dose $1x10^{12}$ ions/cm^2 and $5x10^{12}$ ions/cm^2 are found 3.37 eV, 3.17 eV and 3.44 eV respectively. On the basis of results it is concluded that the absorption was found to increase at $1x10^{12}$ ions/cm^2 and decrease at $5x10^{12}$ ions/cm^2 for both type samples of TiO_2 and TiO_2/ITO photoanode. However the $1x10^{12}$ ions/cm^2 ion irradiated N719 dye loaded TiO_2 film has shown comparatively high absorption. Hence it is concluded that $1x10^{12}$ ions/cm^2 dose of oxygen ion irradiated TiO_2 thin film sample loaded with N719 dye may enhance the efficiency of dye sensitized solar cell.

But in the case of ITO film as a photoelectrode the transmission is reported to decrease with increase in oxygen ion fluence upto $1x10^{12}$ ions/cm^2 which indicates low performance of DSSC.

Acknowledgements

Financial and experimentally support from Inter-University Accelerator Centre (an autonomous centre of UGC), New Delhi (India) is gratefully acknowledged.

References

1. Regan, B.O.; Gratzel, M.; *Nature* **1991**, 353**,** 737. **DOI:** 10.1038/353737a0
2. Thavasi, V.; Renugopalakrishnan, V.; Jose, R.; Ramakrishna, S.; *Mat. Sci. and Eng.* **2009**, 3, 81. **DOI:** 10.1016/j.mser.2008.09.001
3. Knickerbocker, S.A.; Kulkarni, A.K.; *J. Vac. Sci. Technol. A* **1995,** 13 (3), 1048. **DOI:** 10.1116/1.579583
4. Bendonia, R; Barthélémyc, A; Sangiorgia, N.; Sangiorgia, A.; Sansona, A. ; *J. of Photochem. and Photobio. A: Chem.* 2016, 330, 8–14. **DOI:** 10.1016/j.jphotochem.2016.07.021
5. Kim, S.B.; Park, J.; Kim, C.; Okuyama, K.; Lee, S.; Jang, H.; Kim, T.; *J. Phys. Chem. C*, **2015**, 119 (29), 16552–16559. **DOI:** 10.1021/acs.jpcc.5b02309
6. Fujishima, A.; Honda, K.; *Nature* **1972,** 238. **DOI:** 10.1038/238037a0
7. Weinberger, B. R.; Garber, R. B.; *Appl. Phys. Lett.* **1995**, 66, 2409. **DOI:** 10.1063/1.113956
8. Park, J.H.; Kim, S.; Bard, A. J.; *Nano Lett*, **2006,** 6, 24. **DOI:** 10.1021/nl051807y
9. Kongkanad, A.; Dominguez, R. M.; Kamat, P. V.; *Nano Lett.* **2007**, *7*, 676. **DOI:** 10.1021/nl0627238.
10. Hwang, Y.; Boukai, A.; Yang , P.D.; *Nano Lett.* **2009**, 9, 410. **DOI:** 10.1021/nl8032763
11. Ren, W.; Ai, Z.; Jia, F.; Zhang, L.; Fan, X.; Zou, Z.; *Appl. Catal.B: Environ.* **2007,** *69*, 138. **DOI**: 10.1016/j.apcatb.2006.06.015
12. Elfanaoui, A.; Elhamri, E.; Boulkaddat, L.; Ihlal, A.; Bouabid, K.; Laanab, L; Taleb, A.; Portier, X.; *Int. J. of Hydrogen Ener.* **2011**, *36*, 4130. **DOI**: 10.1016/j.ijhydene.2010.07.057
13. Avasthi, , D.K.; *Current science*, **2000**, *78*, 1297, **DOI:** 10.1016/j.apcatb.2006.06.015
14. Fink, D.; Chadderton, L. T.; *Braz. J. Phys.* **2005,** *35***,** 735. **DOI:** 10.1590/S0103-97332005000500003
15. Semwal, A; Negi, A; Sonkwade R.G.; Rana JMS, Romala, R.C.; *Indian J. of pure and Applied Phys.*, **2010**, *48*, 496. **DOI:** 10.1177/1420326X11419983
16. Singh, H.K.; Agarwal, D.C.; Chavhan; P.M.; Mehra, R.M.; Aggarwal, S.; Kulriya, P.K.; Tripathi, A.; Avasthi, D.K.; *Nucl. Inst. and Methods in Phys. Research B* **2010,** *268*, 3223. **DOI:** 10.1016/j.nimb.2010.05.094
17. Gokulakrishnan , V.; Parthiban, S.; Elangovan,E.; Jeganathan, K.; Kanjilal, D.; Asokan, K.; Martins, R.; Fortunato, E.; Ramamurthi, K.; *Phys. and Chem.* **2012,** *81*, 589. **DOI**: 10.1016/j.radphyschem.2012.02.037
18. Kumar, V.; Jain, A.; Pratap, D.; Agarwal, D.C.; Sulania; Kumar, V.V.S.; Tripathi, A., Varma, S.; Chauhan, R.S.; *Adv. Mat. Lett.* **2013**, 4(6), 428. **DOI**: 10.5185/amlett.2012.ib.108
19. Agarwal, D.C.; Kumar, A.; Khan, S.A.; Kabiraj, D.; Singh, F.; Tripathi, A.; Pivin, J.C.; Chauhan, R.S.; Avasthi, D.K. *Nucl. Instr. Meth. B*. **2006,** *244*, 136. **DOI:** 10.1016/j.nimb.2005.11.077
20. Mehta, G. K.; *Nucl. Instr. and Meth. B*. **2006**, *212*, 8. **DOI:** 10.1016/S0168-583X(03)01835-4
21. Avsthi, D. K.; Pivin, J.C.; *Ion Current Sci.* **2010,** *98*, 780.
22. Agarwal, D. C. ; Chauhan, R.S.; Avasthi, D. K.; Khan, S. A.; Kabiraj, D.; Sulania; I. J. *Appl. Phys.* **2008,** *104*, 024304. **DOI**: 10.1063/1.2953177
23. Tripathi, N.; Rath,S.; *ECS Journal of Solid State Sci. and Tech.* **2014**, *3*, 21. **DOI:** 10.1149/2.002403jss
24. Zhengcao, L.; Teng, Y.; *Applied Surface Sci*., **2015,** *327*, 478. **DOI:** 10.1016/j.apsusc.2014.12.009
25. Breese, M., *Addison-Wesley*, Reading, Mass: USA, **2013**. **DOI:** 10.1177/1028315313496572
26. Mir, F.A ; Batoo, K.M. ; *App. Physics A*, **2016**, *122*, 418. **DOI:** 10.1007/s00339-016-9948-3
27. Patel, G.B.; Singh, N.L., Kulriya, P.K. *Nucl. Instr. Meth. B.: Beam Interactions with Mat. and Atoms***, 2016**, *379*, 156. **DOI:** 10.1016/j.nimb.2016.04.018
28. Wesch, W.; Wendler, E. Ion Beam Modification of Solids: Ion-Solid Interaction and Radiation Damage; Springer : Netherlands, **2016**. **DOI:** 10.1007/978-3-319-33561-2
29. Avasthi**,** D.K.; Mehta**;** G.K. Swift Heavy Ions for Materials Engineering and Nanostructuring; Springer Series in Materials Science; Springer: Netherlands, **2011**. **DOI:** 10.1007/978-94-007-1229-4
30. Maarof1, S.K.M.; Abdullah1, S.; Rusop, M.; *Mat. Scie. and Eng*. **2013**, 46, 012009 **DOI**: 012009doi:10.1088/1757-899X/46/1/012009
31. Ziegler, J. F., Biersack, J., Littmark, U; Pregamon Press, NewYork, **1985**.
32. Deshpande, N.G.; Sagade, A.A.; Chavhan, S.D.; Vyas, J.C.; Singh, F.; Tripathi, A.K.; *Vacuum*, **2008**, 82, 39. **DOI**: 10.1016/j.vacuum.2007.03.004
33. Deshpande, N.G.; Gudage, Y.G.; Ghosh, A.; Vyas, J.C.; Singh, F.; Tripathi, A.; Sharma, R.J.; *Phys. D: Appl. Phys*. **2008**, 41, 035308. **DOI:** 10.1088/0022-3727/41/3/035308
34. Bringa, E. M.; Johnson; *Phys. Review Letters* **2002,** *88(16*, 165501. **DOI**: 10.1103/PhysRevLett.88.165501
35. Cullity, B.D., Elements of X-Ray Diffraction; Addison-Wesley, Reading, Mass : USA, **1956**. **DOI:** 10.1021/ed034pA178
36. Smith, R.A., Semiconductors; Cambridge University Press: Cambridge, **1978.** **DOI**: 10.1177/002072097901600432
37. Moss, T.S. Optical properties of semi-conductors, a semiconductor monograph; Butterworths : London, **1959**. **DOI:** 10.1016/0022-3697(59)90017-4
38. Singh, A.P.; Kumari,S.; Tripathi, A.; Singh, F.; Gaskell, K.J.; Shrivastav, R.; Dass, S.; Ehrman, S.H.; Satsangi, V. *J. ; Phys. Chem*. **2010,** *114*, 622. **DOI:** 10.1021/jp0484938
39. Gokulakrishnan, V.; Parthiban, S.; Elagovan,E.; Ramamurthi, K.; Jeganathan, K.; Kanjilal, D.; Asokan, K.; Martins, R.; Fortunato, E.; *Nucl. Instr. Meth.Phys. B*. **2011**, *269*, 1836. **DOI**: 10.1016/j.nimb.2011.05.008
40. Kumar, V.; Singh, R. G.; Purohit, L. P.; Singh, F.; *Adv. Mat. Lett*. **2013**, *4*, 423. **DOI:** 10.5185/amlett.2012.ib.107
41. Manavizadeh, N.; Boroumand, F.A.; Asl-Soleimani, E.; *Thin Solid Films* **2009,** *517*, 2324. **DOI:** 10.1016/j.tsf.2008.11.027